

Impact of surface morphology above threading dislocations on leakage current in 4H-SiC diodes

Hirokazu Fujiwara,^{1,a)} Hideki Naruoka,¹ Masaki Konishi,¹ Kimimori Hamada,¹ Takashi Katsuno,² Tsuyoshi Ishikawa,² Yukihiko Watanabe,² and Takeshi Endo³

¹Toyota Motor Corporation, Toyota, Aichi 470-0309, Japan

²Power Electronics Research Division, Toyota Central R&D Laboratories Inc., Nagakute, Aichi 480-1192, Japan

³Research Laboratories, DENSO CORPORATION, Nisshin, Aichi 470-0111, Japan

(Received 2 May 2012; accepted 9 July 2012; published online 24 July 2012)

The nano-scale pits above the threading dislocations were found to be in the same location as the leakage current points in Schottky barrier diodes and junction barrier Schottky diodes. This study compared the leakage current of 1.2 kV, 200 A diodes with and without nano-scale pits. The leakage current in diodes without nano-scale pits was lower than those in diodes with pits. In the diodes without nano-scale pits, the leakage currents were generated at step-bunching area and the leakage current at the threading dislocations was not observed. © 2012 American Institute of Physics. [<http://dx.doi.org/10.1063/1.4738886>]

Superior properties of silicon carbide (SiC) make this material an attractive candidate for fabricating power devices with high breakdown voltage and lower power loss. High-current and high-voltage capabilities are a key requirement for the introduction of SiC power devices in the electric vehicle, hybrid vehicle (HV), and fuel cell vehicle applications. SiC diodes used in HV systems have a rated current of several hundred Ampere and an active size of at least 25 mm². As the active size increases, however, product yield deteriorates dramatically due to the greater leakage current in reverse IV characteristics and decreasing breakdown voltage.¹ It is widely recognized that micro-pipe, carrot, comet, triangle, and stacking fault such as crystalline defects in SiC epitaxial wafer cause increasing leakage current and deteriorating breakdown voltage in SiC power devices.^{1–7} SiC epitaxial wafers have high density of threading screw dislocations (TSDs), threading edge dislocations (TEDs), and basal plane dislocations. In recent years, TSD and TED can be distinguished easily by using a laser microscope.⁸ The influence of threading dislocations on the performance of diodes has been also investigated.^{1,9–18} TSDs and TEDs in SiC p-n junction diodes (PNDs) lead to the onset of micro-plasma at slightly lower reverse voltage than theoretical breakdown voltage.^{9–11} Almost all of leakage current points in PND corresponded to TSD positions by the analysis of emission microscopy. These TSDs were defined as killer defects in PND with a high concentration of aluminum (Al) of $2 \times 10^{20} \text{ cm}^{-3}$.¹⁴ However, it is not clear how threading dislocation affect the reverse IV characteristics in the Schottky barrier diodes (SBDs) and junction barrier Schottky diodes (JBSDs). As described in the previous report, a positive correlation has been identified between leakage current density and threading dislocation density in SBDs and JBSDs when the reverse voltage is applied.¹⁸ The surface morphologies of leakage current sources of SBD were analyzed using atomic force microscopy (AFM); additionally, nano-sized circular cone shaped pits

above threading dislocations were observed at the leakage current points in Schottky junction regions of SBD and JBSD.^{17,18} Although studies have been made on the influence of nano-scale pits, the evidence for supporting this mechanism which leakage current is generated by nano-scale pits is exiguous. Therefore, the purpose of this study was to compare the leakage currents of diodes with and without nano-scale pits and to identify the mechanism of increasing leakage current in nano-scale pits above threading dislocations.

SBDs and JBSDs were fabricated on a 4H-SiC (0001), 3-in. N-type wafer. The thickness of drift layer was 13 μm and the donor concentration was $5 \times 10^{15} \text{ cm}^{-3}$. Molybdenum (Mo) and nickel (Ni) contacts were used for the anode and cathode electrode, respectively. After forming each contact by vapor deposition, post-annealing processes were performed for the Mo contact at 800 °C or more and for the Ni contact at 1000 °C or more. P+ layer at PN junction regions with an acceptor concentration of $1 \times 10^{19} \text{ cm}^{-3}$ and a depth of 700 nm in the JBSD were formed by Al ion implantation. In the same way, Al ion implantation was used to form the junction termination extension and field limiting ring at the edge termination structures. Diodes with active area of 25 mm² were located within a chip size of $6 \times 6 \text{ mm}^2$, and a total of 5 SBD and 30 JBSD chips with a rated current of 200 A were fabricated on a same wafer. In order to verify the impact of threading dislocations, SBDs and JBSDs were fabricated by two different processes. These diodes with and without nano-scale pits are referred to as samples A and B, respectively, thus two wafers with same specifications were used in this study. Sample A was fabricated by the conventional process,¹⁹ resulting in the formation of nano-scale pits above the threading dislocations on the SiC drift layer surface. Sample B was fabricated without the formation of nano-scale pits by a planarization process.

The impact of surface morphology on the leakage current density in reverse IV characteristics of diodes was investigated as follows. The reverse IV characteristics were evaluated at room temperature. Next, after removing the cathode electrode by mechanical polishing, the leakage

^{a)}Electronic mail: fujiwara@hirokazu.tec.toyota.co.jp. Tel.: +81-565-46-3397. FAX: +81-561-46-3382.

points on application of a reverse voltage of -1200 V were analyzed by emission microscopy. The leakage points were marked to an accuracy of $\pm 2 \mu\text{m}$ using a focused ion beam. Then, after removing the anode electrode by a sulfuric acid and hydrogen peroxide mixture before a hydrofluoric acid treatment, the surface morphology of the leakage points was scanned using tapping mode of AFM, and three-dimensional nano-scale irregularities image was obtained. Finally, the threading dislocation density was evaluated by a laser microscope after defect-selective etching using a potassium hydroxide (KOH) alkaline solution.

The diodes with and without nano-scale pits were fabricated in order to verify the impact of nano-scale pits directly above threading dislocations on the leakage current of diodes. Figure 1 shows the typical reverse IV characteristics of samples A and B in 30 JBSDs. The leakage current density in sample A increased suddenly to approximately 10^{-6} A/cm^2 at -100 V, varied from $1 \times 10^{-5} \text{ A/cm}^2$ to $2 \times 10^{-4} \text{ A/cm}^2$ at -1200 V, and was convex reverse IV characteristic. In contrast, the leakage current density in sample B was extremely low and was 10^{-8} A/cm^2 at -100 V. Even at -1200 V, the leakage current density remained low within a variation range of $2 \times 10^{-7} \text{ A/cm}^2$ to $3 \times 10^{-6} \text{ A/cm}^2$. The reverse IV characteristic of sample B was a straight line. The leakage current density of sample B at -1200 V was reduced by roughly two orders of magnitude compared to sample A. Similarly, in the case of the SBDs, the leakage currents in sample A were found to be higher than those in sample B. The distributions of barrier height, and drift layer donor concentration and thickness were investigated in a whole wafer. The barrier heights of samples A and B were almost same at $1.14 \pm 0.01 \text{ eV}$ and $1.17 \pm 0.01 \text{ eV}$, respectively. The drift layer donor concentration and thickness in samples A and B were also same (sample A: $5.4 \times 10^{15} \text{ cm}^{-3}$ and $13.0 \mu\text{m}$, sample B: $5.1 \times 10^{15} \text{ cm}^{-3}$ and $13.3 \mu\text{m}$). In other words, the difference in the leakage current density in samples A and B cannot be explained based on the differences

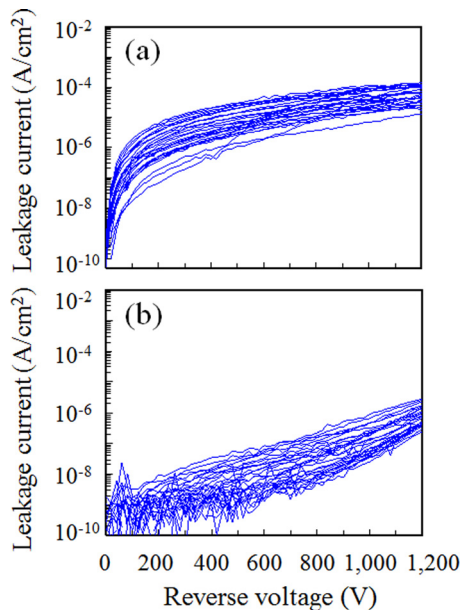


FIG. 1. Reverse IV characteristics of 200 Å JBSDs: (a) sample A with nano-scale pits and (b) sample B without pits.

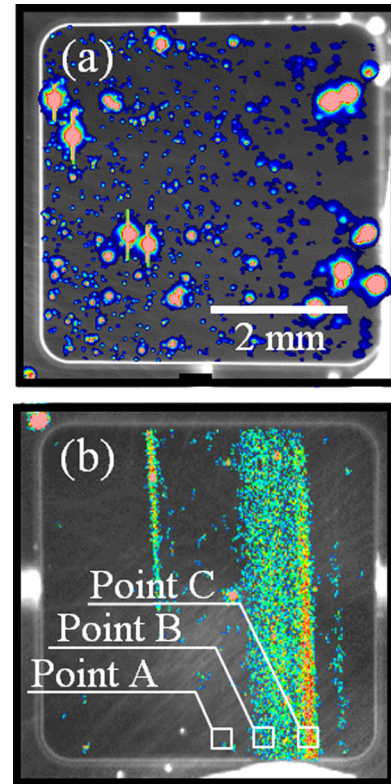


FIG. 2. Emission microscopy images corresponding to leakage points in 200 Å SBDs: (a) sample A with nano-scale pits and (b) sample B without pits. The scales in (a) and (b) are same.

in the barrier height, or on the differences in the drift layer donor concentration or thickness.

Figure 2 represents emission points that show leakage current positions of SBDs in samples A and B at -1200 V as identified by emission microscopy. In the case of sample A, the leakage points are uniformly scattered within the active area. In contrast, the leakage points in sample B have a vertically striped pattern and leakage current occurs locally. Figure 3 shows the detailed surface morphology of the same sample shown in Fig. 2(a). Fig. 3(a) shows the leakage points at the upper left quarter of the active area in sample A, which measured by a high sensitivity emission microscopy. Figs. 3(b) and 3(c) shows an optical micrograph and AFM image at point 1 in Fig. 3(a). Inverted cone-shaped nano-scale pits with a diameter of approximately 200 nm , a depth of

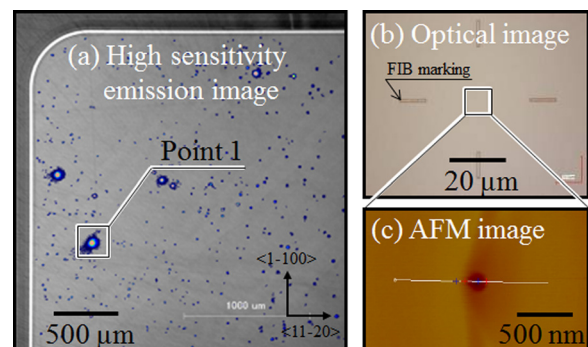


FIG. 3. Surface morphology of sample A with nano-scale pits in Fig. 2(a): (a) high sensitivity emission microscopy image, (b) optical micrograph, and (c) AFM image at point 1 in (a).

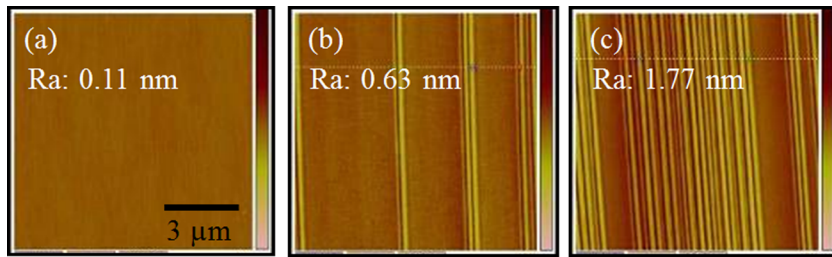


FIG. 4. Surface morphology of sample B without nano-scale pits measured by AFM in Fig. 2(b): (a) point A, (b) point B, and (c) point C.

approximately 25–45 nm, and a peak angle of 135° were found at the leakage points. The distribution of threading dislocation (KOH etching pit) density in the whole wafer was from 2.9×10^3 to $96 \times 10^3/\text{cm}^2$, and the average was $38 \times 10^3/\text{cm}^2$. In sample A, The positions of nano-scale pits correspond to the positions of threading dislocations, which were identified by KOH etching. The most important factor of leakage current generation in sample A is the surface morphology of threading dislocations rather than the presence of threading dislocations. Figure 4 shows the surface morphology of points A, B, and C in Fig. 2(b) measured by AFM. The point A is a normal area without the emission points and has very smooth surface. After KOH etching, however some TEDs and TSDs were observed in the surface. In contrast, the points B and C have weak emission and comparatively strong emission points, respectively. Fine step-bunching (a series of peaks and valleys) were observed in points B and C. The maximum height of Rmax (peak to valley) and the surface roughness of Ra in point B are 8 nm and 0.63 nm, respectively. The Rmax and Ra in point C are 10 nm and 1.77 nm, respectively. The origination of step-bunching is thought to be occurred during epitaxial growth. Since the nano-scale pits were removed in the process for sample B, it is assumed that leakage current was subsequently generated by electric field concentration in the valleys of the step-bunching area where the surface is rough. However, the electric field concentration and leakage current in the step-bunching area are less than that produced by the nano-scale pits.

Figure 5 shows the impact of presence of nano-scale pits on the leakage current analyzed by device simulation.²⁰ The leakage current density was calculated with and without nano-scale pits using a thermal field-emission model.²¹ Assuming a barrier height of 1.2 eV, a tunneling electron effective mass of $0.25 m_0$, a nano-scale pit depth of 45 nm, a pit peak angle of 135° , and a pit density of $35\,400/\text{cm}^2$. With nano-scale pits,

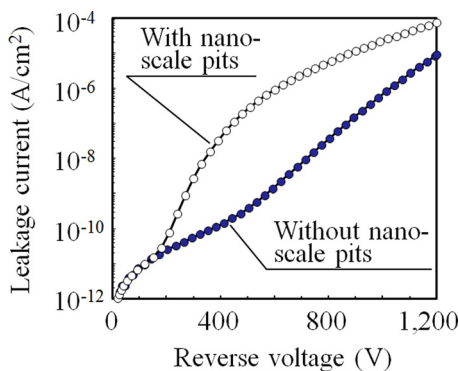


FIG. 5. Comparison of theoretical reverse IV curves with and without nano-scale pits. These data are referenced from Ref. 20.

electric field concentration several times larger than that generated with a flat Schottky interface occurred at the nano-scale pit peaks. As a result, the leakage current density at -200 V suddenly increased, forming a clearly convex-shaped IV characteristic. The magnitude of leakage current at -1200 V was also found to be greater for samples with nano-scale pits. This is in agreement with the experimental results obtained for samples with nano-scale pits as shown in Fig. 1(a). In contrast, without nano-scale pits, the leakage current density increased linearly with respect to the reverse voltage, the same as that obtained without nano-scale pits in Fig. 1(b). Consequently, the nano-scale pit has a more major impact on leakage current than its own dislocation crystalline defect in Schottky junction interface of SBD and JBSD, which identified by the simulation analysis and experimental results.

In summary, this study examined the impact of nano-scale pits above threading dislocations on the leakage current in 4H-SiC SBDs and JBSDs, and identified the mechanism by which nano-scale pits generated the leakage current. When nano-scale pits above threading dislocations were present, the leakage current with a low applied voltage increased suddenly, forming an abnormal convex reverse IV characteristic. In contrast, the leakage current of diodes without nano-scale pits increased slightly and were lower than these of diodes without pits with nano-scale pits, despite the presence of threading dislocation crystalline defects. In the case of diodes with nano-scale pits, the leakage current increased because the electric field concentrated at the nano-scale pit peaks was several times larger than those in diodes without pits. In the case of diode without nano-scale pits, moreover, the leakage currents were mainly generated at the step-bunching area.

The authors would like to thank T. Ohnishi and A. Adachi of Toyota Motor Corporation and T. Morino and T. Yamamoto of Denso Corporation for helpful discussions. The authors also would like to thank M. Iida and A. Mikami of Toyota Motor Corporation for the measurements of emission microscopy.

¹H. Fujiwara, M. Konishi, T. Ohnishi, T. Nakamura, K. Hamada, T. Katsuno, Y. Watanabe, T. Endo, T. Yamamoto, K. Tsuruta, and S. Onda, *Mater. Sci. Forum* **679–680**, 694 (2011).

²T. Kimoto, N. Miyamoto, and H. Matsunami, *IEEE Trans. Electron Devices* **46**(3), 471 (1999).

³P. G. Neudeck, *Mater. Sci. Forum* **338–342**, 1161 (2000).

⁴D. T. Morissette and J. A. Cooper, *Mater. Sci. Forum* **389–393**, 1133 (2002).

⁵R. A. Berechman, M. Skowronski, and Q. Zhang, *J. Appl. Phys.* **105**, 074513 (2009).

⁶H. Fujiwara, T. Kimoto, T. Tojo, and H. Matsunami, *Appl. Phys. Lett.* **87**, 051912 (2005).

⁷T. Katsuno, Y. Watanabe, H. Fujiwara, M. Konishi, T. Yamamoto, and T. Endo, *Jpn. J. Appl. Phys., Part 1* **50**, 04DP04 (2011).

⁸T. Katsuno, Y. Watanabe, H. Fujiwara, M. Konishi, T. Yamamoto, and T. Endo, *Mater. Sci. Forum* **679–680**, 298 (2011).

- ⁹P. G. Neudeck, W. Huang, and M. Dudley, *Solid-State Electron.* **42**, 2157 (1998).
- ¹⁰R. A. Berechman, M. Skowronski, S. Soloviev, and P. Sandvik, *J. Appl. Phys.* **107**, 114504 (2010).
- ¹¹F. Zhao, M. M. Islam, B. K. Daas, and T. S. Sudarshan, *Mater. Lett.* **64**, 281 (2010).
- ¹²Q. Wahab, A. Ellison, C. Hallin, A. Henry, J. Di Persio, R. Martinez, and E. Janzén, *Mater. Sci. Forum* **338–342**, 1175 (2000).
- ¹³H. Saitoh, T. Kimoto, and H. Matsunami, *Mater. Sci. Forum* **457–460**, 997 (2004).
- ¹⁴T. Tsuji, T. Tawara, R. Tanuma, Y. Yonezawa, N. Iwamuro, K. Kosaka, H. Yurimoto, S. Kobayashi, H. Matsuhata, K. Fukuda, H. Okumura, and K. Arai, *Mater. Sci. Forum* **645–648**, 913 (2010).
- ¹⁵B. A. Hull, J. J. Sumakeris, M. J. O’Loughlin, J. Zhang, J. Richmond, A. R. Powell, M. J. Paisley, V. F. Tsvetkov, A. Hefner, and A. Rivera, *Mater. Sci. Forum* **600–603**, 931 (2008).
- ¹⁶A. Grekov, Q. Zhang, H. Fatima, A. Agarwal, and T. Sudarshan, *Microelectron. Reliab.* **48**, 1664 (2008).
- ¹⁷T. Katsuno, Y. Watanabe, H. Fujiwara, M. Konishi, H. Naruoka, J. Morimoto, T. Morino, and T. Endo, *Appl. Phys. Lett.* **98**, 222111 (2011).
- ¹⁸H. Fujiwara, T. Katsuno, T. Ishikawa, H. Naruoka, M. Konishi, T. Endo, Y. Watanabe, and K. Hamada, *Appl. Phys. Lett.* **100**, 242102 (2012).
- ¹⁹T. Yamamoto, J. Kojima, T. Endo, E. Okuno, T. Sakakibara, and S. Onda, *Mater. Sci. Forum* **600–603**, 939 (2008).
- ²⁰T. Ishikawa, T. Katsuno, Y. Watanabe, H. Fujiwara, and T. Morino, “Critical density of nano-scale pits for suppressing variability in leakage current of SiC Schottky barrier diodes,” in *Proceedings of International Symposium on EcoTopia Science 2011, Nagoya, Japan, 9–11 December 2011*, edited by K. Kitagawa, G. Obinata, and O. Takai (Nagoya University, Japan), p. 306.
- ²¹T. Hatakeyama, M. Kushibe, T. Watanabe, S. Imai, and T. Shinohe, *Mater. Sci. Forum* **433–436**, 831 (2003).